Phase behavior of water–menthol based deep eutectic solvent–dodecane system

4 authors:

Papu Kumar Naik
Indian Institute of Technology Guwahati
28 PUBLICATIONS **362** CITATIONS

Debashis Kundu
Indian Institute of Technology Guwahati
31 PUBLICATIONS **440** CITATIONS

Priyotosh Bairagya
Jadavpur University
4 PUBLICATIONS **28** CITATIONS

Tamal Banerjee
Indian Institute of Technology Guwahati
177 PUBLICATIONS **4,065** CITATIONS

Some of the authors of this publication are also working on these related projects:

Project MD of Deep Eutectic Solvent with PAH View project

Project Thermal Dehydrogenation of Amine Borane Complexes View project

Phase behavior of water-menthol based deep eutectic solvent-dodecane system

Papu Kumar Naik [a,1], Debashis Kundu [b,1], Priyotosh Bairagya [c], Tamal Banerjee [a,*]

[a] Department of Chemical Engineering, Indian Institute of Technology Guwahati, Guwahati, Assam 781039, India
[b] Department of Chemical Engineering, Institute of Chemical Technology Marathwada Campus, Jalna, India
[c] Department of Chemical Engineering, Jadavpur University, Kolkata, West Bengal 700032, India

ARTICLE INFO

ABSTRACT

In the current work, two menthol-based hydrophobic deep eutectic solvents (DESs) have been synthesized to extract dodecane from water-dodecane emulsion at 298 K and atmospheric pressure. The equilibrium mixture produces two biphasic liquid-liquid equilibrium systems and one triphasic liquid-liquid-liquid equilibrium system. ^{1}H NMR has been used to calculate the molar composition of each phase. For both the lauric and decanoic acid-based DES, the extract phase of biphasic region-1 is rich in DES; whereas the raffinate phase is predominantly water. However, for the biphasic region-2, the extract phase is the dodecane rich phase and raffinate phase is the mixture of DES and dodecane having a dominant composition of DES. In case of triphasic region, i.e. top phase consists of dodecane and the bottom phase is only water. The middle phase becomes an emulsion where DES is the dominant component. The selectivity analysis in the triphasic region proves that both the DESs have high selectivity to extract dodecane from the water-dodecane microemulsion. The experimental mole fractions are correlated with genetic algorithm (GA) promoted NRTL and UNIQUAC models to predict the phase behavior. An average overall root means square deviation (RMSD, %) of 0.174% is observed for the biphasic region and 0.048% for the triphasic employing GA-NRTL model. GA-UNIQUAC predicts an average overall RMSD of 0.340% for biphasic regions and 0.129% for the triphasic region.

1. Introduction

Deep Eutectic Solvent (DES) is a new generation solvent prepared from a hydrogen bond donor (HBD) and hydrogen bond acceptor (HBA). The HBDs are generally carboxylic acid, amide, alcohol, amine etc.; whereas HBAs can either be quaternary salt with metal halides or hydrophobic natural compounds. The DES is characterized by the proportionate mixture of HBA and HBD that forms a clear and stable eutectic mixture by the hydrogen bonding (H-bond) interaction and possesses a lower melting point than the individual compounds. The formation of DES depends on the choice of HBA and HBD as well as their molar composition. HBD and HBA are further able to donate and accept the proton respectively and thus prone to form H-bond with solute. Therefore, the combination of these two facilitates the enhanced solvation capability of DES [1–3]. For this reason, DES is being successfully used for the separation process [4]. Apart from that, DES is also used in organic and inorganic synthesis [5], catalysis [6], electrochemistry [7], and green analytical chemistry [8,9]. Hydrophobic DES is a relatively new class

of DES primarily originating from the work of Warrag et al. [10,11]. In the hydrophobic DES, the HBDs are mainly composed of hydrophobicF carboxylic acid i.e. fatty acid or alcohol, and HBAs that are generally natural hydrophobic compounds or quaternary ammonium salt with a longer alkyl chain [11–13]. Among the various classes of hydrophobic DES, menthol-based DES has been successfully applied for the separation processes [14,15].

Water-dodecane system has been used as a model system for water–oil microemulsion. Typically oil (i.e. dodecane) is recovered from water using surfactant [16,17]. Surfactant-water-dodecane is long viewed as the representative of the Treybal type-III as well as the Winsor type-III system. There is a handful example of ionic liquid (IL) using as a surfactant to recover dodecane from water [18–23]. Although ILs produce encouraging results as an entrainer to recover oil from an emulsion, the operating cost of a large scale synthesis of IL creates obstacle from commercial application. From past literature, hydrophobic ionic liquids (ILs) have been known to perform better for the recovery of oil [20–22]. However in many situations, separation from dilute feed stream becomes challenging. It is in this context that the synthesis of low-cost hydrophobic solvent is desired. Due to the high cost and nature of tox-

---

Table 1
Details of chemicals used in this work.

Name of the chemical	CAS registry no.	Purity (%)	supplier	Purification method
Menthol	1490-04-6	≥99 %	Tokyo Chemical Industry	Used as received
Lauric acid	143-07-7	≥98 %	Tokyo Chemical Industry	Used as received
Decanoic acid	334-48-5	≥98 %	Tokyo Chemical Industry	Used as received
n-dodecane	112-40-3	≥99 %	Tokyo Chemical Industry	Used as received
dimethyl sulfoxide-d_6	2206-27-1	≥99.8%	Merck	Used as received

icity, cheaper and sustainable solvents are now being explored. DES is currently known as a cheap, sustainable and also easy to synthesis solvent that gets limited exposure in separation processes as an alternative solvent to IL and organic solvents [24–26]. Most of the DESs proposed so far in the literature have a hydrophilic character and thus are unstable in water, leading to the separation of both components. With respect to the hydrophobicity of the DES, in the current work, DL-menthol and organic acids (lauric, decanoic) have been chosen as HBA and HBD respectively [27,28]. These DESs are known to have favorable solvation properties for polar and nonpolar compounds and are more stable at high temperature and are suitable for the extraction of inorganic and organic compounds [29,30]. Therefore, we have investigated for the first time the recovery of dodecane from the water-dodecane system that is known as Treybal type III and Winsor type III system, using menthol-based DES. The effectiveness of hydrophobic DES has been attempted by measuring the phase behavior. The phase compositions are analyzed by proton Nuclear Magnetic Resonance (^{1}H NMR) spectra. The calculated phase compositions are plotted in ternary diagram to reveal the phase behavior. In addition to that, the experimental dataset is fitted with genetic algorithm (GA) promoted NRTL and UNIQUAC models (GA-NRTL and GA- UNIQUAC) using a modified Rachford-Rice algorithm to compute the model predicted phase behavior.

2. Experimental details

2.1. Chemicals

The chemical compounds of HBDs and HBA, n-dodecane and auxiliary chemicals were procured from commercial sources and were of analytical grade. The purity of chemicals, CAS registry number, name of the supplier and purification methods are given in Table 1. Deionized (DI) water was supplied from an in-house Millipore water synthesis unit (Millipore, model: ELix-3).

2.2. Preparation of DES

Menthol and lauric acid or decanoic acid are mixed in a specific molar ratio to prepare the DES. For DES1, menthol and lauric acid are mixed in 2:1 molar ratio and for DES2 menthol and decanoic acid are mixed in 1:1 molar ratio [14,15]. The respective mixtures are heated at 60 °C in a round bottom flask and are stirred until a clear solution is observed. Here menthol is acting as HBA and lauric acid or decanoic acid as HBD. The clear solution is kept in a vacuum oven at 80 °C for 48 h to remove the volatile matter and water content. Karl Fischer Titrator (Metrohm, 787 KF Titrino, Switzerland) is used to measure the water content in the vacuum dried DESs. The water content of DES1 is found to be 0.917 wt% and 0.874 wt% for DES2. The measured water content of DES2 is substantially lower than the reported water content of 2.17 wt% by Dietz et al. [24] The densities of the produced DESs are measured at atmospheric pressure by digital density-meter (Anton Paar DMA 4500) having an uncertainty of ±0.001 g cm^{-3} (Table 2). The measured density of DES2 is 0.896 g cm^{-3} and Dietz et al. [24] report the density as 0.8976 g cm^{-3}. Therefore the reduction in density is by 0.18% which mainly refers to the lower water content of DES2 synthesized in this work. Later the vacuum dried solution is characterized with ^{1}H NMR for the composition analysis (600 MHz NMR, Bruker, Germany).
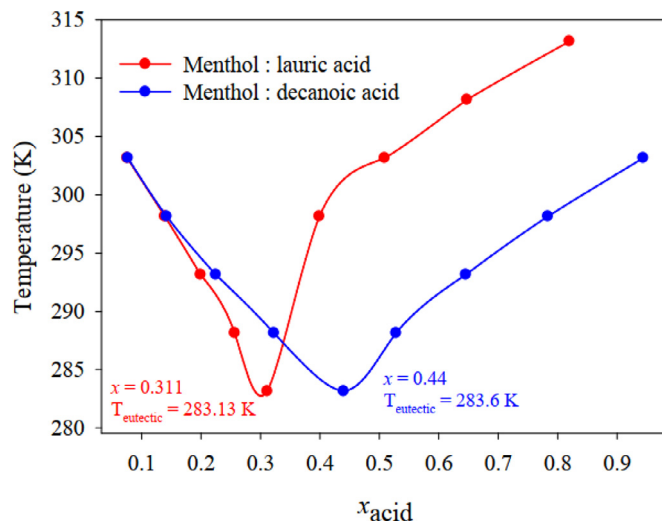

Fig. 1. COSMO-SAC predicted eutectic composition of DES composed of lauric/decanoic acid with menthol.
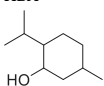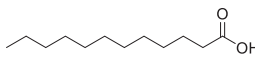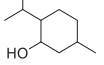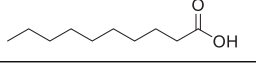
2.2.1. Selection of molar ratio of HBA and HBD for DES formation

It should be noted that all molar ratios will not produce a eutectic point or a liquid phase for forming DES. Liquid formation takes place only at the eutectic point or the ratio which is 2:1 for lauric acid (DES1) and 1:1 for decanoic acid (DES-2). Eutectic point is the point of lowest temperature and optimal molar ratio, where both phases co-exist. This could be very specific for all different types of DES combination of HBA and HBD. However, molar ratios other than the 1:1 and 2:1 do not yield a liquid phase on account of the existence of the solid phase. Thus, the case of DES1, DL-menthol and lauric acid are mixed in a molar ratio of 2:1 to get the eutectic point composition. Similarly, DL-menthol and decanoic acid are mixed in a molar ratio of 1:1 to form DES2. This can be estimated through quantum chemical calculations and adopting a statistical-based approach such as Conductor like Screening Model Segment Activity Coefficient model (COSMO-SAC) [31,32]. This selection of molar ratio can be better explained in our earlier work [14,33]. The eutectic point of the DES2 is predicted at x= 0.44, where x corresponds to the mole fraction of decanoic acid (Fig. 1). This essentially implies a molar ratio of 0.56/0.44 (HBA:HBD) ∼1. Lauric acid is another organic acid having a longer carbon chain as compared to decanoic acid. The COSMO-SAC predicts to be at x= 0.311 where x corresponds to the mole fraction of lauric acid. This essentially implies a molar ratio of 0.689/0.311 ∼2 (HBA:HBD). This ratio, therefore, corresponds to the working liquid temperature of the DES. Thus based on the COSMO-SAC predictions of the eutectic point, the appropriate mole ratio of HBA:HBD is chosen.

2.3. Phase equilibrium experiment

The phase equilibrium experiments are conducted by preparing adequate mixtures of the three components in 10 mL stoppered bottle. The net volume of the DES in each composition is maintained at 5 mL. The feed volumes of respective compounds are computed according to

Table 2
DES synthesized in this work.

Name	HBA:HBD	HBA	HBD	Density[a] (g cm⁻³)
DES1	2:1			0.894
DES2	1:1			0.896

[a] Density measured at T = 298.15 K. Standard uncertainty: $u(T)$ = 0.05 K, $u(\rho)$ = 0.001 g cm⁻³

the corresponding molecular weight, density and proportion of the individual compound. Finally, the feed compositions of water-dodecane-DES systems have been reported in terms of component mole fractions and provided in Table S1 of supplementary information (SI). However, the vacuum-dried DESs themselves contain 0.917 wt% and 0.874 wt% (DES1 and DES2 respectively) water and these water contents are duly taken into consideration during the preparation of solution for the phase equilibrium measurement. Various combinations of mole fractions of water, dodecane and DES are tried. However, for all the mole fractions, the mixtures are not forming a ternary or binary mixture. Therefore, only those initial feed compositions are shown where the biphasic or triphasic phase equilibrium is observed. Eight compositions are chosen in such a way that they cover all the biphasic and triphasic regions. Afterward, the mixture is kept inside an incubator shaker (Daihan LabTech, China) for rapid mixing at 298 K, 200 rpm for 6 h. The mixtures are then allowed to settle for 12 h at 298 K to obtain a clear and stable phase separation. Thereafter, the samples of different phases are collected by syringe and are dissolved in dimethyl sulfoxide-d₆. The corresponding compositions are analyzed using ¹H NMR (Bruker, AVANCE III HD, and software Topspin 3.5). Fig. S1 represents the digital image of biphasic and triphasic behavior of water-DES-dodecane system.

¹H NMR has widely been studied for the analysis of phase compositions in multicomponent mixtures [4,25,26,34,35]. The detailed justification of using NMR to analyze the phase compositions over other techniques such as HPLC, is given in supplementary material. The reproducibility of the NMR-derived mole fractions is checked on known mixtures of dodecane-DES1 and water-DES1 and it is found that the mole fractions remained within the uncertainty range of ±0.001. The number of hydrogen atoms corresponding to a moiety is calculated with the measured area under each of the resonances. Therefore, the mole fraction of each component is calculated with the corresponding area of a hydrogen atom to the total calculated area in the spectra. Mathematically, it is given as,

$$x_i = \frac{H_i}{\sum_{i=1}^{3} H_i} \tag{1}$$

Where, H_i signifies the corresponding resonance area of the proton and x_i is the mole fraction for single hydrogen of ith component of the mixture. The degree of affinity of solute with extract and raffinate phases is calculated by the distribution ratio (D_i). A large value of distribution ratio implies a lower amount of solvent is required with respect to the feed. Selectivity (S_{ij}) is the ratio of distribution ratio of solute and solvent of original solution (not the extractant). Therefore, for the useful extraction process, it must be greater than 1. The higher value of selectivity is desirable for the selection of solvent [36,37]. The mathematical forms are given by,

$$D_i = \frac{x_i^{Extract}}{x_i^{Raffinate}} \tag{2}$$

$$S_{ij} = \frac{x_i^{Extract}}{x_i^{Raffinate}} / \frac{x_j^{Extract}}{x_j^{Raffinate}} \tag{3}$$

Here, $x_i^{Extract}$ and $x_i^{Raffinate}$ represent the mole fractions of ith component i.e. dodecane and $x_j^{Extract}$ and $x_j^{Raffinate}$ represent the mole fractions of jth component i.e. water at extract and raffinate phases respectively.

2.4. Estimation of uncertainty of measurement

For the experimental uncertainty, the experiments are replicated and the mean and standard deviation (σ) are calculated. With this data the standard uncertainty (u) is obtained by the following equation:

$$u = \frac{\sigma}{\sqrt{n}} \tag{4}$$

Where n is the sample size (e.g. for ten number of repetitive measurement; n = 10). For the pressure, instrumental factory rating and measurement error are simultaneously considered and the uncertainty is calculated with the above method. In addition to that, the calculation for temperature uncertainty considers the degree of equilibration, position of the thermometer and its calibration [38]. The detail discussion is given in supplementary material and the data is tabulated in Table S2. The standard uncertainty of pressure is 0.01 MPa or 10 kPa, standard uncertainty of temperature is 0.05 K, standard uncertainty for density is 0. 001 g.cm⁻³ and the standard uncertainty of mole fractions do not exceed 0.001. It is to be noted that due to the baseline correction of the NMR spectra, concentrations lower than 0.001 are very difficult to obtain. This usually signifies the uncertainty levels of the NMR spectra for the calculation of mole fraction composition.

2.5. Correlated models for the experimental dataset

Modified Rachford-Rice (R-R) algorithm is used to predict the phase behavior. The R-R algorithm invokes genetic algorithm (GA) based NRTL and UNIQUAC models abbreviated as GA-NRTL and GA-UNIQUAC models to calculate the activity coefficients. The mole fractions are subsequently calculated with the activity coefficients. The details of NRTL, UNIQUAC and modified R-R algorithm are given in detail in the literature [39,40]. First Principle-based Polarizable Continuum Model (PCM) is used to determine the volume and surface parameters of UNIQUAC models and is given in Table S3 of SI. The excess Gibbs energy models require binary interaction parameters which are bounded by lower and upper limits. The GA searches the optimum values of the binary interaction parameters of NRTL and UNIQUAC models by using the objective function. The objective function equation is regressed from the experimental ternary compositions. This is necessary due to the fact that the GA tends to maximize a function. The R-R framework calls activity coefficient models which use the binary interaction parameters generated by the GA formulation. The detailed calculation procedure of GA to find the interaction parameters of NRTL and UNIQUAC are discussed in the literature [41]. The binary interaction parameter (A_{ij}) is calculated for both NRTL and UNIQUAC model and given in Tables

S4,S5 of supplementary material.

$$F_{\left(\begin{array}{c} with\ respect\ to\ Aij \\ where\ i,j=1,2,3 \\ and\ \ j \neq i \end{array}\right)} = -\sum_{i=1}^{c}\sum_{j=1}^{p}\sum_{t=1}^{m}\left(x_{calc,i,t}^{j} - x_{expt,i,t}^{j}\right)^2 \tag{5}$$

The accuracy of the prediction with respect to the experimental values is calculated via root-mean-square-deviation (*RMSD*). It is defined as:

$$RMSD(\%) = 100 \times \left[\sum_{i=1}^{c}\sum_{j=1}^{p}\sum_{t=1}^{m}\frac{\left(x_{calc,i,t}^{j} - x_{expt,i,t}^{j}\right)^2}{mcp}\right]^{1/2} \tag{6}$$

Where m refers to the number of tie-lines, c refers to the number of system components and p denotes the number of phases. $x_{expt,i,t}^{j}$ and $x_{calc,i,t}^{j}$ are experimental and predicted mole fractions.

3. Results and discussions

3.1. ^1H NMR analysis

^{1}H NMR spectra of DES1 and DES2 are shown in Fig. S2 of SI. The number of hydrogen of the corresponding moiety is determined by calculating area under the resonance and dividing the area with a single hydrogen atom. In a spectrum, the total area of all hydrogen is normalized. Only one prominent resonance peak is chosen for the single component of the mixture for quantification of the corresponding mole fraction in the respective phase. The detailed calculation steps can be found in our previous literature [4,29]. Chemical shift at $\delta = 0.83$–0.84 ppm (denoted by a_1) is assigned to the –CH_3 moiety of menthol whereas the chemical shift at $\delta = 0.70$–0.71 ppm (denoted by b_1) is assigned to the terminal –CH_3 moiety of lauric acid (Fig. S2(i)). The –CH_2 moieties of lauric acid are obtained at $\delta = 1.22$ ppm (denoted by b_2) and $\delta = 1.82$ ppm (denoted by b_3). The –OH moiety of both lauric acid and menthol are obtained at $\delta = 4.35$ ppm (denoted by a_3). Chemical Shift at $\delta = 1.47$, 2.15–2.16 and 3.14 ppm (denoted by a_4, a_2, a_6, respectively) represent the hydrogen belong to the ring of menthol. In a similar manner, Fig. S2(ii) represents ^{1}H NMR of DES2. The location of –CH_3, -CH_2 and –OH moieties are in very similar position to that of the Fig. S2(i).

Fig. S3 of SI represents the ^{1}H NMR spectra of the upper and bottom phase of the biphasic region-1 for system-1 (water + DES1 + dodecane). In Fig. S3(i), the chemical shift at $\delta = 0.70$–0.71 ppm represents the terminal –CH_3 moiety of lauric acid and dodecane (denoted by b_1 and c_1, respectively), The peak c_1 is used for the quantification of dodecane in upper phase. However, the chemical shift of –CH_3 moieties of menthol is observed at $\delta = 0.84$ ppm. The chemical shift at $\delta = 1.22$ ppm (denoted by b_2 and c_2) represents the –CH_2 moiety of lauric acid and dodecane. In presence of dodecane, there is a marginal downfield shift of –OH moiety at $\delta = 4.40$ ppm (denoted by 'd_1'). However, other resonances of menthol remain in a similar position to that of pure DES1. However, in the bottom phase of biphasic region-1, only chemical shift –OH moiety is observed at $\delta = 3.98$ ppm (Fig. S3(ii)). Therefore, the bottom phase solely contains water. This implies that DES1 can extract the entire dodecane from the emulsion. However, the ^{1}H NMR of biphasic region-2 of system-1 shows the separation of dodecane in the top phase and water-free DES1 rich bottom phase (Fig. S4 of SI). In Fig. S4(i), the chemical shift at $\delta = 0.91$ and 1.29 ppm represent the –CH_3 and –CH_2 moieties respectively. The corresponding chemical moieties of DES1 and dodecane are observed in a similar position to that of respective pure compounds in the ^{1}H NMR spectra at Fig. S4(ii).

Fig. S5 of supplementary material represents the ^{1}H NMR characterization of triphasic LLLE behavior. The resonance spectra of top phase reflects the chemical shift of –CH_3 and –CH_2 moiety of dodecane (denoted by c_1 and c_2). This implies that in the triphasic LLLE, dodecane is the sole component in the top phase. Similarly, in the bottom phase

Table 3

Composition of the experimental liquid-liquid equilibrium and liquid–liquid–liquid equilibrium tie-line data for the ternary system water + DES1 + dodecane, at temperature (*T*) 298 K and pressure (*P*) 0.1 MPa. The molar fractions of water, DES1 and dodecane are represented by x_1, x_2 and x_3, respectively.[a]

Biphasic region-1					
Upper phase			Bottom phase		
x_1	x_2	x_3	x_1	x_2	x_3
0.069	0.931	0.000	1.000	0.000	0.000
0.043	0.902	0.055	1.000	0.000	0.000
0.033	0.885	0.082	1.000	0.000	0.000
0.029	0.852	0.119	1.000	0.000	0.000
Biphasic region-2					
Upper phase			Bottom phase		
x_1	x_2	x_3	x_1	x_2	x_3
0.000	0.000	1.000	0.000	0.702	0.298
0.000	0.000	1.000	0.005	0.785	0.210
0.000	0.000	1.000	0.014	0.835	0.151
Triphasic region								
Upper phase			Middle phase			Bottom phase		
x_1	x_2	x_3	x_1	x_2	x_3	x_1	x_2	x_3
0.000	0.000	1.000	0.041	0.808	0.151	1.000	0.000	0.000

Standard uncertainties (*u*): $u(P) = 10$ kPa, $u(T) = 0.05$ K, $u(x) = 0.001$

[a] DES composition as per Table 2, $u(x) = 0.001$

Table 4

Composition of the experimental liquid-liquid equilibrium and liquid–liquid–liquid equilibrium tie-line data for the ternary system water + DES2 + dodecane, at temperature (*T*) 298 K and pressure (*P*) 0.1 MPa. The molar fractions of water, DES2 and dodecane are represented by x_1, x_2 and x_3, respectively.[a]

Biphasic region-1					
Upper phase			Bottom phase		
x_1	x_2	x_3	x_1	x_2	x_3
0.034	0.966	0.000	1.000	0.000	0.000
0.037	0.879	0.084	1.000	0.000	0.000
0.039	0.837	0.124	0.993	0.007	0.000
0.041	0.808	0.151	0.989	0.012	0.000
Biphasic region-2					
Upper phase			Bottom phase		
x_1	x_2	x_3	x_1	x_2	x_3
0.000	0.002	0.998	0.000	0.792	0.208
0.000	0.005	0.995	0.015	0.790	0.195
0.000	0.009	0.991	0.021	0.799	0.180
Triphasic region								
Upper phase			Middle phase			Bottom phase		
x_1	x_2	x_3	x_1	x_2	x_3	x_1	x_2	x_3
0.000	0.002	0.998	0.058	0.789	0.153	0.996	0.004	0.000

Standard uncertainties (*u*): $u(P) = 10$ kPa, $u(T) = 0.05$ K, $u(x) = 0.001$

[a] DES composition as per Table 2, $u(x) = 0.001$

(Fig. S5(iii)), the sole presence of water is observed. The spectral analysis proves an emulsion in the middle phase. However, the composition analysis from Table 3 shows the middle phase is DES1 rich phase. The resonance due to methyl moiety of menthol (∼0.84 ppm) has been used for the quantification of DES1. Therefore, in the triphasic LLLE region, DES1 is able to separate dodecane and water emulsion into two distinct phases which can be easily separated.

The ^{1}H NMR of biphasic region-1 (LLE) of system-2 (water + DES2 + dodecane) is given in Fig. S6 of SI. It is observed from Table 4 that the compositional analysis of the upper phase of biphasic region-1 of system-2 in DES2 rich phase has a trace amount of water and dodecane. The chemical shift at Fig. S6(i) shows the corresponding resonances of various moieties of DES2, dodecane and water. These resonances are observed at a very similar position to that of pure compounds. A large chemical shift of –OH moiety is observed in Fig. S6(ii) which indicates the dominant presence of water in the bottom phase of biphasic region-1. The corresponding compositional analysis shown in Table 4 reveals the trace amount of presence of DES2 where the corresponding chemical shifts are observed in Fig. S6(ii). Fig. S67of SI rep-

resents the ^{1}H NMR of biphasic region-2 of system-2. The resonance of the top phase shows the presence of DES and dodecane, whereas in the bottom phase all three compounds are present. However, from the compositional analysis in Table 4, dodecane is observed as a pure form in the upper phase in a couple of tielines. From Table 4, it is visible that unlike the DES1, DES2 is not able to completely separate water from dodecane in the biphasic region. Due to the lower hydrophobicity of decanoic acid, the resonances of DES2 are also visible in the bottom phase (Fig. S7(ii)).

The ^{1}H NMR of the triphasic region of system-2 is given in Fig. S8 of supplementary material. However, unlike the biphasic region, DES2 facilitates complete separation of dodecane to top phase and water in the bottom phase. The presence of corresponding resonances of DES2, dodecane and water in the middle phase confirms the DES is present as the dominant emulsion layer. However, in the triphasic region, DES2 is also able to extract dodecane from water.

3.2. LLE and LLLE phase behavior

Based on the ^{1}H NMR analysis, the mole fraction of water, dodecane and DES are calculated for each phase and tabulated in Tables 3 and 4. The DES facilitated phase equilibrium divides oil-water emulsion i.e. water-dodecane system into two biphasic regions. The biphasic region-1 is predominantly DES-water equilibrium, where the upper phase (extract) is DES-rich phase due to the lower density of menthol-based DES. For system-1, the bottom phase (raffinate) of biphasic region-1 is entirely water. However, complete separation is not observed for the case of system-2 in Table 4. A trace amount of DES2 is also obtained in the bottom phase (raffinate) of biphasic region-1 of system-2. However, for both DES systems, a trace amount of water and dodecane are also found in the upper phase (extract) of biphasic region-1. The biphasic region-2 is predominantly DES-dodecane equilibrium. Due to lower density, dodecane is found in the upper phase of biphasic region-2. At the upper phase of biphasic region-2, a trace amount of DES2 is obtained which is not the case for DES1. The complete separation of water and dodecane is achieved in the bottom phase of biphasic region-1 and upper phase of biphasic region-2 respectively with the DES1. Therefore, it can be concluded that the hydrophobicity of DES certainly improves the extraction efficiency. The distribution of dodecane in biphasic region-1 of both the systems cannot be calculated and as per Eq. (3), a low value of distribution ratio of water is calculated. However, in the biphasic region-2, the extract phase almost entirely consists of dodecane and water is absent. Further, raffinate phase is predominantly DES with a minor presence of dodecane. Therefore, the calculated distribution ratio of dodecane at biphasic region-2 is given in Table 5. All the distribution ratio values are greater than unity reflecting menthol-based DESs are capable of separating dodecane from water in the biphasic region-2. The absence of distribution ratios in either biphasic region implied that selectivity cannot be calculated for biphasic regions.

Among the DESs, high values of selectivity are reported for DES1 (Table 5). This indicates that DES1 has a preferential ability to separate dodecane and water compared to DES2. Also, the separation factor decreases as the concentration of dodecane in the feed increases. This is primarily due to the reduction of the two-phase region with the increase in the concentration of dodecane. A similar pattern is also seen for the distribution coefficient which refers to the amount of solvent required for the desired separation. As the DES is hydrophobic, the mole fraction is negligible in the raffinate phases. Also, lauric acid is an organic acid having a longer carbon chain as compared to decanoic acid. Hence, in the case of DES1, hydrogen bonding interaction may be enhanced with the incoming dodecane than DES2. This is due to the fact that possessing a higher charge density results in a higher fraction of active site for initiating hydrogen bonding. Therefore, DES1−dodecane nonbonded interaction is stronger than DES2−dodecane system.

Further, the biphasic regions are separated by a triphasic region where the middle phase of triphase is DES enriched emulsion phase con-

Table 5
Calculation of for distribution ratio and selectivity.

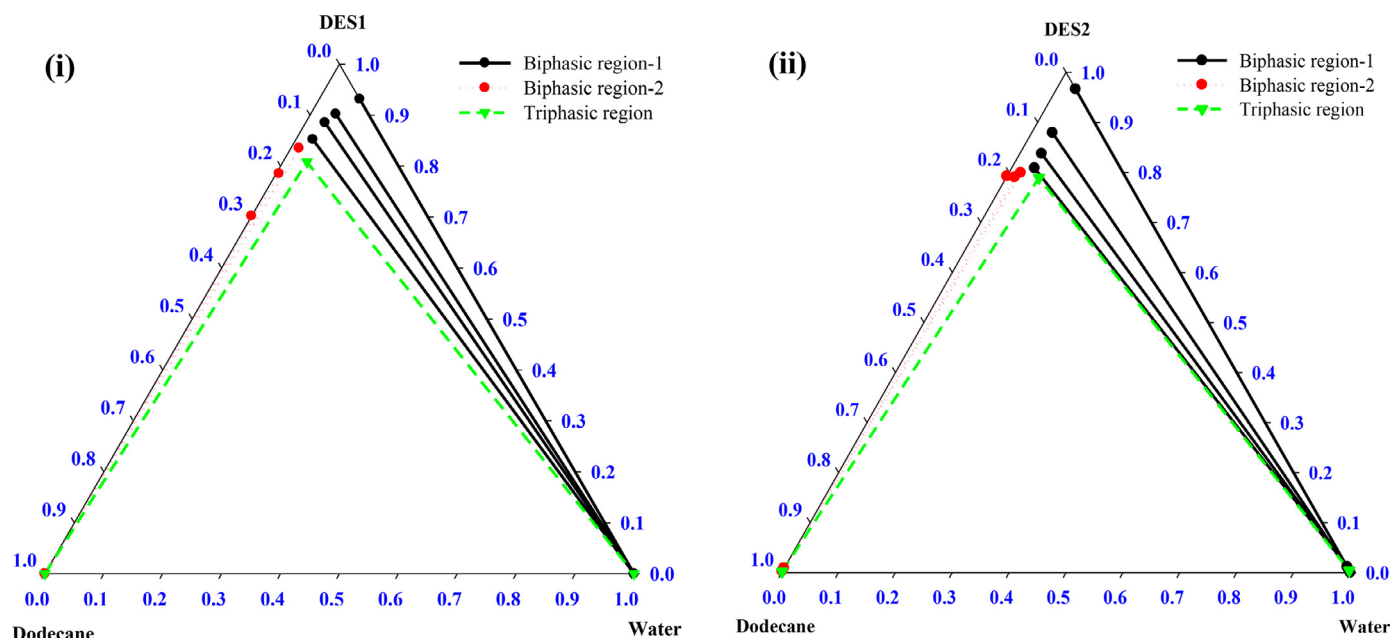| System Parameter		System-1: water-DES1-dodecane		System-2: water-DES2-dodecane	
		$D_{dodecane}$	D_{water}	$D_{dodecane}$	D_{water}
Distribution ratio	Biphasic region-1	NA	0.069	NA	0.034
		NA	0.043	NA	0.037
		NA	0.033	NA	0.039
		NA	0.029	NA	0.041
	Biphasic region-2	3.356	NA	4.798	NA
		4.762	NA	5.103	NA
		6.667	NA	5.506	NA
	Triphasic region	6.623 (calculated between top and middle phase)	0.041 (calculated between top and middle phase)	6.523 (calculated between middle and bottom phase)	0.058 (calculated between middle and bottom phase)
Selectivity		161.537		112.466	

Fig. 2. Experimental phase diagram of the ternary systems (i) water + DES1 + dodecane system at 298.15 K and pressure P = 0.1 MPa (ii) water + DES2 + dodecane system at 298.15 K and pressure P = 0.1 MPa.

taining less than 22% dodecane and water combined. The middle phase is surrounded by a clear top phase of dodecane and the bottom phase of water. The biphasic and triphasic regions of system-1 and system-2 are given in Fig. 2. It is observed that for both the systems large triphasic envelope separates the two biphasic regions. Further, the phase envelope of biphasic region-1 is larger than the phase envelops of biphasic region-2 for both systems. In the triphasic region, DES separates dodecane and water at the top and bottom phases keeping itself in the middle phase. Therefore, the distribution ratio of dodecane is calculated between the top and middle phases and that of water is calculated between middle and bottom phases. Therefore, for system-1, the selectivity is calculated 161.537 and for system-2, it is 112.466. The higher value of selectivity implies that DES1 is better capable of extracting dodecane from the microemulsion than DES2.

The amphiphilic nature of DES creates three partially miscible liquid pairs resulting in a ternary system that is classified as the Treybal type III system. However, the triphasic region is surrounded by two biphasic regions. For that, the definition of the Winsor type III system is also applicable for water-DES-dodecane systems. Furthermore, the triphasic region has excess oil (i.e. dodecane) and water phase along with the surfactant (i.e. DES) rich phase. This is particularly suitable for enhanced oil recovery (EOR) application where surfactant (DES here) separates the oil (i.e. dodecane) from water. The large triphasic envelope is surrounded by the two biphasic regions. The hydrophobicity of DES increases with the length of the alkyl chain of HBDs. In all cases, it is clear that the concentration of DES is zero in the upper biphasic region and lower triphasic region. Also, it is noted that the upper triphasic region contains the only dodecane in both systems. It suggests that the hydrophobicity of the DES makes the extraction possible and the dodecane is extracted in a pure separate layer in the triphase. This indicates that DES acts as a good solvent for the extraction of dodecane from the water-dodecane emulsion.

The mixtures of oil (dodecane) and DES are separated into two phases shortly after mixing. This reveals that both DESs are very less miscible with the oil used in this study and do not cause stable emulsions with it. Hence, they will not mix spontaneously and easily get separated. The small fraction of DES phase of the biphasic regions is contaminated with hydrocarbon but it can be reused in successive cycles. Addition-

ally from Table S1, it is evident that phase equilibrium composition can be in biphasic region-1, biphasic region-2 or triphasic region. For both the DESs, it can be observed from Table 3; the DES is able to separate the dodecane from microemulsion if the feed composition of DES lies within 0.50 mole fractions and the mole fractions water-dodecane are more than 0.25 individually. Due to the cheaper price of the precursor of DES compares to that of ILs, large amount usage of DES is economical. Further, the separation efficiency increases in the triphasic region which is further visible from Table 5. Therefore, separation of DES from the hydrocarbon stream is relatively easy if the feed compositions are kept in biphasic region-1 or triphasic region.

3.3. NRTL and UNIQUAC model predicted phase behavior of LLE and LLLE systems

The experimentally measured mole fractions are correlated in GA-NRTL and GA-UNIQUAC models to predict the biphasic and triphasic behavior. The predicted biphasic and triphasic behaviors are given in Fig. 3 and the corresponding RMSDs are given in Tables S6 and S7 of SI, respectively. Due to the presence of water in DES, enhanced interactions are reported by Dietz et al. [24] and to model the phase behavior by PC-SAFT model, the authors have considered the additional binary interaction parameters (k_{ij}). However, here we have modeled the experimental phase behavior with GA-NRTL and GA-UNIQUAC models. The binary interaction parameters are predicted by GA algorithm. Therefore, the presence of water content in the DES will not lead to additional parameter optimization. The GA algorithm will fit the interaction parameters as per the experimental mole fractions of the compositions. The application of GA in NRTL and UNIQUAC yield very low RMSD for both the DESs in the biphasic and triphasic behavior. An average overall RMSD of 0.174% for two DESs in the LLE regions and 0.048% for the LLLE region are predicted by GA-NRTL. GA-UNIQUAC predicts an average overall RMSD of 0.340% for LLE regions and 0.129% for the LLLE region. The binary interaction parameters are given in Tables S4 and S5. The correlation results open up the future possibilities of designing extraction equipment for the water-DES-dodecane system.
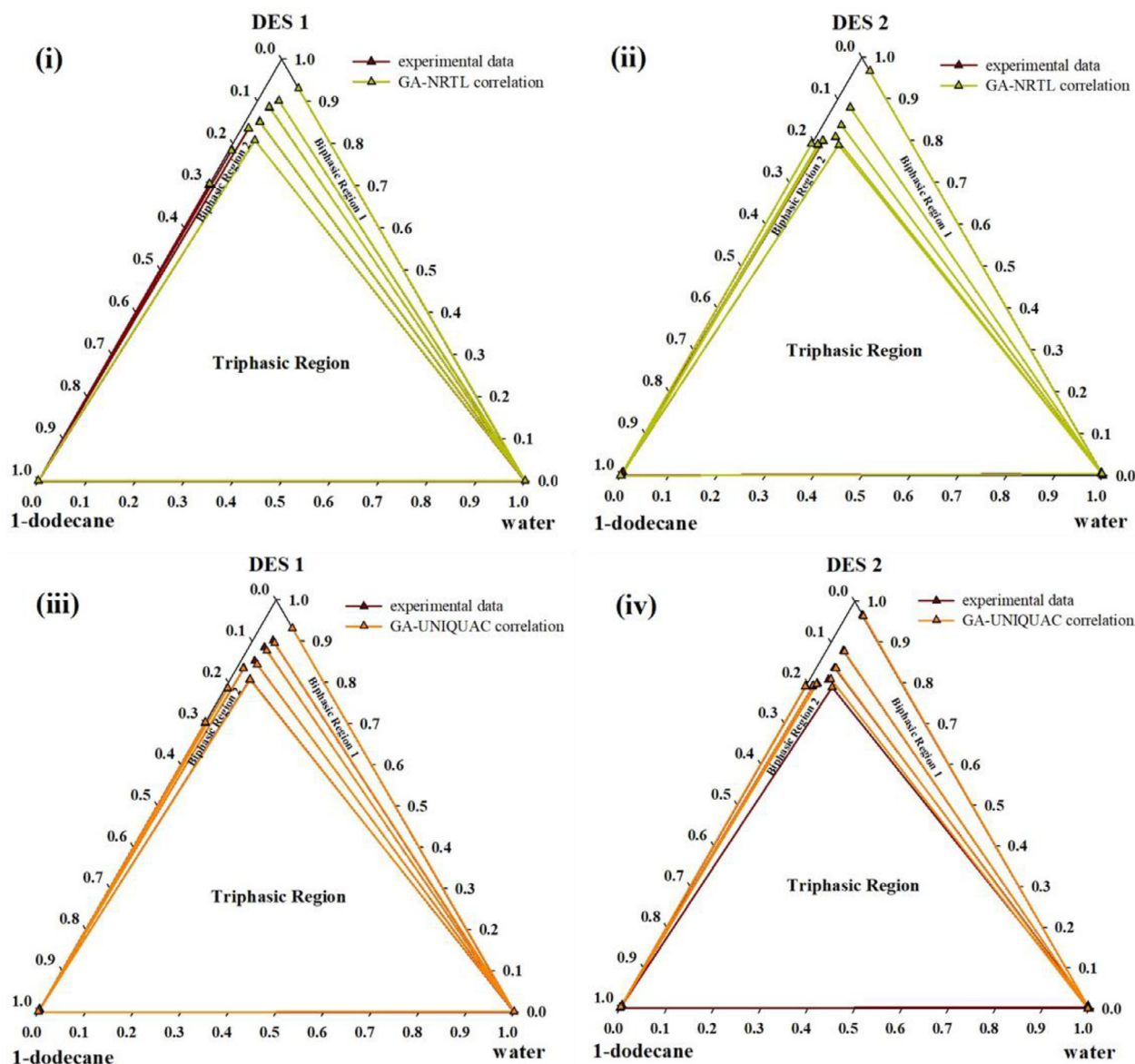
Fig. 3. Ternary phase diagrams of experimental and correlated phase compositions using GA-NRTL algorithm (i,ii) and GA-UNIQUAC algorithm (iii,iv).

3.4. Comparison of phase behavior with IL facilitated systems

As DES is reported first time for the extraction of dodecane from the microemulsion, we compare the biphasic and triphasic behavior with the IL facilitated systems. Trihexyl(tetradecyl)phosphonium cation in combination with chloride, dicyanamide, bis(2,4,4-trimethylpentyl) phosphinate, bis(trifluoromethylsulfonyl)imide anion based ILs are used to extract dodecane from water-dodecane system [18,20–23]. In all of the cases, Winsor type III phase behavior is observed for water-IL-dodecane systems i.e. triphasic behavior is surrounded by the biphasic region. The extractions are possible without the addition of a co-surfactant. For the surfactant flooding applications, the interfacial tensions between equilibrium phases of the binary and ternary systems are determined in the presence or absence of salt. Rodríguez-Palmeiro et al. [19] employ PC-SAFT model to reveal the LLLE behavior of the water-IL-dodecane system using 1-decyl-3-methylimidazolium bis(trifluoromethylsulfonyl)imide and 1-dodecyl-3-methylimidazolium bis(trifluoromethylsulfonyl)imide ILs. The hydrophobic nature of ILs is particularly suitable for the complete removal of dodecane from emulsion and the imidazolium based ILs produce better extraction efficiency

over the trihexyl(tetradecyl)phosphonium cation based ILs. In the similar manner, menthol-based hydrophobic DES produces excellent recovery of dodecane from the emulsion and the biphasic and triphasic behavior are successfully correlated with GA-NRTL and GA-UNIQUAC models. Therefore, comparing the present work with the IL-based literature, it can be concluded that DES can effectively replace IL in separating oil (i.e. dodecane) from water-oil (i.e. water-dodecane) mixture.

4. Conclusion

Menthol-based DES with lauric acid and decanoic acid as HBDs are synthesized with an aim of extracting of dodecane from the water-dodecane mixture. Mole fractions of components in every phase are successfully calculated from ^{1}H NMR data. The water-DES-dodecane systems yield two biphasic regions and one triphasic region making these systems Treybal type III as well as Winsor type III systems. In the triphasic region, dodecane and water are completely separated in top and bottom phases respectively implying the menthol-based DES can extract dodecane from an emulsion. This can also be viewed from the phase behavior of the biphasic region. The calculation of selectivity in

the triphasic region produces that lauric acid-based DES1 has a selectivity of 161.537 which is greater than the decanoic acid-based DES2. The higher selectivity proves that DES1 has a better extraction ability of dodecane and requires in a lower amount than DES2 for the extraction process. Therefore, the cost-effective menthol-based hydrophobic DES can be used for EOR application and could potentially replace expensive IL.

Declaration of Competing Interest

The authors declare that they have no known competing financial interests or personal relationships that could have appeared to influence the work reported in this paper.

Acknowledgment

The authors acknowledge the Central Instrument Facility of the Indian Institute of Technology Guwahati for providing the NMR facility.

Supplementary materials

Supplementary material associated with this article can be found, in the online version, at doi:10.1016/j.ctta.2021.100011.

Reference

[1] E.L. Smith, A.P. Abbott, K.S. Ryder, Deep eutectic solvents (DESs) and their applications, Chem. Rev. 114 (2014) 11060–11082, doi:10.1021/cr300162p.

[2] Q. Zhang, K.D.O. Vigier, S. Royer, F. Jerome, Deep eutectic solvents: syntheses, properties and applications, Chem. Soc. Rev. 41 (21) (2012) 7108–7146, doi:10.1039/C2CS35178A.

[3] C. Florindo, L.C. Branco, I.M. Marrucho, In the quest for green solvents design: from hydrophilic to hydrophobic (deep) eutectic solvents, ChemSusChem 12 (2019) 1549–1559, doi:10.1002/cssc.201900147.

[4] P.K. Naik, S. Paul, T. Banerjee, Liquid liquid equilibria measurements for the extraction of poly aromatic nitrogen hydrocarbons with a low cost deep eutectic solvent: experimental and theoretical insights, J. Mol. Liq. 243 (2017) 542–552, doi:10.1016/j.molliq.2017.08.044.

[5] M.C. Gutiérrez, D. Carriazo, A. Tamayo, R. Jiménez, F. Picó, J.M. Rojo, M.L. Ferrer, F. del Monte, Deep-eutectic-solvent-assisted synthesis of hierarchical carbon electrodes exhibiting capacitance retention at high current densities, Chem. Eur. J. 17 (2011) 10533–10537, doi:10.1002/chem.201101679.

[6] L. Wei, Y.J. Fan, N. Tian, Z.Y. Zhou, X.Q. Zhao, B.W. Mao, S.G. Sun, Electrochemically shape-controlled synthesis in deep eutectic solvents: a new route to prepare Pt nanocrystals enclosed by high-index facets with high catalytic activity, J. Phys. Chem. C 116 (2012) 2040–2044, doi:10.1021/jp209743h.

[7] M. Figueiredo, C. Gomes, R. Costa, A. Martins, C.M. Pereira, F. Silva, Differential capacity of a deep eutectic solvent based on choline chloride and glycerol on solid electrodes, Electrochim. Acta 54 (2009) 2630–2634, doi:10.1016/j.electacta.2008.10.074.

[8] A. Shishov, A. Bulatov, M. Locatelli, S. Carradori, V. Andruch, Application of deep eutectic solvents in analytical chemistry. A review, Microchem. J. 135 (2017) 33–38, doi:10.1016/j.microc.2017.07.015.

[9] Y. Dai, J. van Spronsen, G.J. Witkamp, R. Verpoorte, Y.H. Choi, Natural deep eutectic solvents as new potential media for green technology, Anal. Chim. Acta 766 (2013) 61–68, doi:10.1016/j.aca.2012.12.019.

[10] S.E. Warrag, C.J. Peters, M.C. Kroon, Deep eutectic solvents for highly efficient separations in oil and gas industries, Curr. Opin. Green Sustain. Chem. 5 (2017) 55–60, doi:10.1016/j.cogsc.2017.03.013.

[11] D.J. van Osch, L.F. Zubeir, A. van den Bruinhorst, M.A. Rocha, M.C. Kroon, Hydrophobic deep eutectic solvents as water-immiscible extractants, Green Chem. 17 (2015) 4518–4521, doi:10.1039/C5GC01451D.

[12] A.K. Dwamena, Recent advances in hydrophobic deep eutectic solvents for extraction, Separations 6 (2019) 9, doi:10.3390/separations6010009.

[13] C. Florindo, L. Romero, I. Rintoul, L.C. Branco, I.M. Marrucho, From phase change materials to green solvents: hydrophobic low viscous fatty acid–based deep eutectic solvents, ACS Sustain. Chem. Eng. 6 (2018) 3888–3895, doi:10.1021/acssuschemeng.7b04235.

[14] R. Verma, M. Mohan, V.V. Goud, T. Banerjee, Operational strategies and comprehensive evaluation of menthol based deep eutectic solvent for the extraction of lower alcohols from aqueous media, ACS Sustain. Chem. Eng. 6 (2018) 16920–16932, doi:10.1021/acssuschemeng.8b04255.

[15] R. Verma, T. Banerjee, Liquid–liquid extraction of lower alcohols using menthol-based hydrophobic deep eutectic solvent: experiments and COSMO-SAC predictions, Ind. Eng. Chem. Res. 57 (2018) 3371–3381, doi:10.1021/acs.iecr.7b05270.

[16] J.L. Salager, A.M. Forgiarini, J. Bullón, How to attain ultralow interfacial tension and three-phase behavior with surfactant formulation for enhanced oil recovery: a review. Part 1. Optimum formulation for simple surfactant–oil–water ternary systems, J. Surfactants Deterg. 16 (2013) 449–472 10.1007/s11743-013-1470-4..

[17] J.L. Salager, A.M. Forgiarini, L. Márquez, L. Manchego, J. Bullón, How to attain an ultralow interfacial tension and a three-phase behavior with a surfactant formulation for enhanced oil recovery: a review. Part 2. Performance improvement trends from Winsor's premise to currently proposed inter- and intra-molecular mixtures, J. Surfactants Deterg. 16 (2013) 631–666, doi:10.1007/s11743-013-1485-x.

[18] I. Rodriguez-Escontrela, I. Rodriguez-Palmeiro, O. Rodriguez, A. Arce, A. Soto, Liquid–liquid–liquid equilibria for water+[P66614][DCA]+ dodecane ternary system, Fluid Phase Equilib 405 (2015) 124–131, doi:10.1016/j.fluid.2015.07.022.

[19] I. Rodríguez-Palmeiro, O. Rodríguez, A. Soto, C. Held, Measurement and PC-SAFT modeling of three-phase behavior, Phys. Chem. Chem. Phys. 17 (2015) 1800–1810, doi:10.1039/C4CP04336G.

[20] S. Lago, M. Francisco, M. Arce, A. Soto, Enhanced oil recovery with the ionic liquid trihexyl (tetradecyl) phosphonium chloride: a phase equilibria study at 75 °C, Energy Fuels 27 (2013) 5806–5810, doi:10.1021/ef401144z.

[21] S. Lago, H. Rodríguez, K. M., A.S Khoshkbarchi, A. Arce, Enhanced oil recovery using the ionic liquid trihexyl (tetradecyl) phosphonium chloride: phase behavior and properties, RSC Adv. 2 (2012) 9392–9397, doi:10.1039/C2RA21698A.

[22] I. Rodríguez-Escontrela, I. Rodríguez-Palmeiro, O. Rodríguez, A. Arce, A. Soto, Phase behavior of the surfactant ionic liquid trihexyltetradecylphosphonium bis(2,4,4-trimethylpentyl)phosphinate with water and dodecane, Colloids Surf. A 480 (2015) 50–59, doi:10.1016/j.colsurfa.2015.04.002.

[23] S. Lago, B. Rodríguez-Cabo, A. Arce, A. Soto, Water/oil/[P66614][NTf2] phase equilibria, J. Chem. Thermodyn. 75 (2014) 63–68, doi:10.1016/j.jct.2014.02.012.

[24] C.H.J.T. Dietz, A. Erve, M.C. Kroon, M.V.S. Annaland, F. Gallucci, C. Held, Thermodynamic properties of hydrophobic deep eutectic solvents and solubility of water and HMF in them: measurements and PC-SAFT modeling, Fluid Phase Equilib. 489 (2019) 75–82, doi:10.1016/j.fluid.2019.02.010.

[25] P.K. Naik, M. Mohan, T. Banerjee, S. Paul, V.V Goud, Molecular dynamic simulations for the extraction of quinoline from heptane in the presence of a low-cost phosphonium-based deep eutectic solvent, J. Phys. Chem. B 122 (2018) 4006–4015, doi:10.1021/acs.jpcb.7b10914.

[26] M. Mohan, P.K. Naik, T. Banerjee, V.V. Goud, S. Paul, Solubility of glucose in tetrabutylammonium bromide based deep eutectic solvents: experimental and molecular dynamic simulations, Fluid Phase Equilib. 448 (2017) 168–177, doi:10.1016/j.fluid.2017.05.024.

[27] A. Mohsenzadeh, Y. Al-Wahaibi, A. Jibril, R. Al-Hajri, S. Shuwa, The novel use of deep eutectic solvents for enhancing heavy oil recovery, J. Pet. Sci. Eng. 130 (2015) 6–15, doi:10.1016/j.petrol.2015.03.018.

[28] R. Verma, Extraction of lower alcohols using novel hydrophobic deep eutectic mixtures: synthesis, phase equilibria experiments and process economics, Ph. D. Thesis, I.I.T. Guwahati, 2018.

[29] A. Abo-Hamad, M. Hayyan, M.A. AlSaadi, M.A. Hashim, Potential applications of deep eutectic solvents in nanotechnology, Chem. Eng. J. 273 (2015) 551–567, doi:10.1016/j.cej.2015.03.091.

[30] P.K. Naik, Molecular modeling and thermodynamic studies on the selective ex- traction of poly aromatic hydrocarbons from fuel oil using deep eutectic solvents, Ph. D. Thesis, I.I.T. Guwahati, 2019.

[31] P. Bairagya, D. Kundu, T. Banerjee, A-priori prediction of complex liquid-liquid-liquid equilibria in organic systems using a continuum solvation model, Phys. Chem. Chem. Phys. 22 (2020) 22023–22034, doi:10.1039/D0CP03225E.

[32] D. Kundu, P.S. Rao, T. Banerjee, First principle prediction of Kamlet-Taft solvatochromic parameters of deep eutectic solvent using COSMO-RS model, Ind. Eng. Chem. Res. 59 (2020) 11329–11339, doi:10.1021/acs.iecr.0c00574.

[33] R. Verma, P.K. Naik, I. Diaz, T. Banerjee, Separation of low molecular weight alcohols from water with deep eutectic solvents: liquid-liquid equilibria and process simulations, Fluid Phase Equilib. 533 (2021) 112949, doi:10.1016/j.fluid.2021.112949.

[34] P.K. Naik, P. Dehury, S. Paul, T. Banerjee, Evaluation of deep eutectic solvent for the selective extraction of toluene and quinoline at T= 308.15 K and p= 1 bar, Fluid Phase Equilib. 423 (2016) 146–155, doi:10.1016/j.fluid.2016.04.018.

[35] M.R. Shah, R. Anantharaj, T. Banerjee, G.D. Yadav, Quaternary (liquid+ liquid) equilibria for systems of imidazolium based ionic liquid+ thiophene+ pyridine+ cyclohexane at 298.15 K: experiments and quantum chemical predictions, J. Chem. Thermodyn. 62 (2013) 142–150, doi:10.1016/j.jct.2013.02.020.

[36] N.R. Varma, A. Ramalingam, T. Banerjee, Experiments, correlations and COSMO-RS predictions for the extraction of benzothiophene from n-hexane using imidazolium-based ionic liquids, Chem. Eng. J. 166 (2011) 30–39, doi:10.1016/j.cej.2010.09.015.

[37] A. Bharti, T. Banerjee, Enhancement of bio-oil derived chemicals in aqueous phase using ionic liquids: experimental and COSMO-SAC predictions using a modified hydrogen bonding expression, Fluid Phase Equilib. 400 (2015) 27–37, doi:10.1016/j.fluid.2015.04.029.

[38] J.C.G.M. Jcgm, Evaluation of measurement data—guide to the expression of uncertainty in measurement, Int. Organ. Stand. Geneva ISBN 50 (2008) 134 (https://www.bipm.org/documents/20126/2071204/JCGM_100_2008_E.pdf/cb0ef43f-baa5-11cf-3f85-4dcd86f77bd6) Acessed 10th August 2021.

[39] D. Kundu, T. Banerjee, Multicomponent vapor-liquid-liquid equilibrium prediction using an a priori segment based model, Ind. Eng. Chem. Res. 50 (2011) 14090–14096, doi:10.1021/ie201864y.

[40] A. Bharti, D. Kundu, D. Rabari, T. Banerjee, Phase Equilibria in Ionic liquid Facilitated Liquid–Liquid Extractions, 1st ed.,, CRC Press, Boca Raton, 2017.

[41] P. Bairagya, D. Kundu, T. Banerjee, Simplified COSMO-SAC based phase equilibria predictions for extractive distillation of toluene-heptane mixtures using ionic liquids, Asia-Pac. J. Chem. Eng. 15 (6) (2020) e2513, doi:10.1002/apj.2513.